Surface-Modification on Vertical Alignment Layer Using UV-Curable Reactive Mesogens

Sung Min Kim, In Young Cho, Woo Il Kim, Kwang-Un Jeong, Seung Hee Lee*, Gi-Dong Lee[1], Jongho Son[2], Jae-Jin Lyu[2], and Kyeong Hyeon Kim[2]

Polymer Fusion Research Center, Department of Polymer-Nano Science and Technology, Chonbuk National University, Chonju, Chonbuk 561-756, Korea
[1]*Department of Electronics Engineering, Dong-A University, Pusan 604-714, Korea*
[2]*AMLCD Division, Samsung Electronics, Kiheung, Kyunggi-do 449-711, Korea*

Received December 7, 2008; accepted January 4, 2009; published online March 23, 2009

The patterned vertical alignment (PVA) liquid crystal (LC) mode shows a wide viewing angle and a perfect dark state at a normal direction. However, it is inevitable to avoid the formation of disclinations and the movement of defect points during stabilization of LC's reorientation. It is due to fact that the LC directors tilt downward in different directions with collisions between them by the fringe-electric field. Consequently, the transmittance decreases and the response time gets slower. In order to overcome this barrier, the pretilt angles in four different directions are introduced on the substrates utilizing UV-curable reactive mesogen (RM) monomers. According to our studies, concentration of RM, UV curing condition, and applied voltage to the cell are critical to achieve an optimized surface-modified PVA mode which provides the well-defined reorientation of the LCs with respect to an electric field. Moreover, morphological behaviors on surface of substrate depending on curing conditions were investigated in order to confirm the existence of the stabilized polymer.

DOI: 10.1143/JJAP.48.032405

1. Introduction

Flat-panel displays (FPD) have successfully and exponentially expanded their territories in display markets. Because of their principle attractions such as low power consumption, high resolution, thinness, flatness and lightness, liquid crystal displays (LCDs) among them are now most widely used not only for small mobile and laptop computer screens, but also for large size desktop computer and television monitors. Conventional twisted nematic (TN) LCD mode[1,2] has been mainly used to portable displays owing to its high transmittance and low power consumption. However, the TN LCD mode shows a narrow viewing angle so that a number of different LCD modes have been proposed for achieving a wider viewing angle, such as in-plane switching (IPS),[3] fringe-field switching (FFS),[4,5] multi-domain vertical alignment (MVA),[6] and patterned vertical alignment (PVA).[7,8] Particularly, the PVA mode is one of the leading technologies for a large size LC-television because of the highest contrast ratio at the normal direction in addition to the improvement of viewing angle characteristics using a super PVA (S-PVA) technology.[9] In spite of these advantages of the PVA mode, the intrinsic drawbacks of the PVA mode should be solved in order to be more competitive as a LCD mode, such as the relatively high threshold and operating voltages, the low transmittance, the slow response time, and the strong grey scale dependency of response time. To overcome these drawbacks, the surface-modified PVA mode has been proposed[10] to generate multi-directional pretilted LCs through polymerization of UV-curable RM. In the surface-modified PVA mode, there are many factors that influence the optimized electro-optic characteristics: the applied voltages during UV-curing process, the UV curing conditions and the percentages of RM mixed with LCs.

In this paper, we investigated the electro-optic characteristics and behaviors of the surface-modified PVA LC mode depending on the UV-curing conditions and the percentages of RM mixed with LCs.

*E-mail address: lsh1@chonbuk.ac.kr

2. Switching Principle of the PVA Mode

The normalized transmission of light in the PVA cell filled with birefringent LC medium under crossed polarizers can be represented as

$$T/T_0 = \sin^2 2\phi(V) \sin^2[\Gamma(V)/2] \quad (1)$$

where $\phi(V)$ is the voltage-dependent angle between the LC optic axis and the transmission axis of the crossed polarizer, and $\Gamma(V)$ is the voltage-dependent phase difference. In the absence of an electric field, both $\phi(V)$ and $\Gamma(V)$ are zero so that the cell appears to be dark under the cross polarized optical microscopy. With a bias voltage, the vertically aligned LC directors should tilt downward for making conditions of $\phi(V) = \pi/4$ and $\Gamma(V) = \pi$, which can maximize the light efficiency.

Since the patterned common and pixel electrodes in a pixel are arranged alternatively in a conventional PVA mode, an oblique field consisted of a vertical and a horizontal electric field component is generated with the bias voltage. This resulting oblique field in a conventional PVA mode with patterned electrodes in chevron shape induces the downward LC tilting in four different diagonal directions to form multi-domains, as shown in Fig. 1. In order for LCs to tilt downward exactly in the four different diagonal directions, the field directions of horizontal components of the oblique fields should be in the diagonal directions. However, in a conventional PVA pixel structure shown in Fig. 1(a), the interference occurs due to the unwanted electric fields from signal lines as well as from pixel edges. This undesirable electric interference generates collisions between LCs, causing several defect points of defect strength of $S = +1$ with dark disclination lines and a condition of $\phi(V) \neq \pi/4$.[10] The existence of disclination lines and defect points is one of the main reasons for a poor transmittance and a lower response time.

In the PVA mode, theoretically, the rising time τ_{on} strongly depends on the intensity of applied electric fields, while the decaying time τ_{off} relies on the cell gap d, the rotational viscosity γ, and the bend elastic constant K_3. The

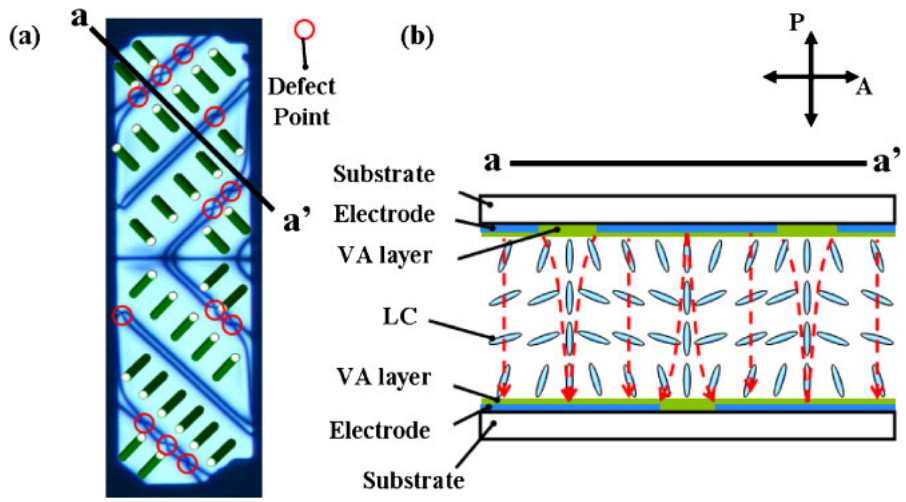

Fig. 1. (Color online) (a) Optical microphotograph of a pixel in the white state of the PVA cell with schematic drawing of LCs and (b) schematic cross-sectional view of the cell along a–a′.

detail relationship between the response time and the cell parameters can be expressed as[11)]

$$\tau_{on} = \tau_{off}/[(V/V_{th})^2 - 1] \quad (2)$$

$$\tau_{off} = \gamma d^2/\pi^2 K_3 \quad (3)$$

where V is applied voltage, and V_{th} is the threshold voltage. Based on eq. (2), it is obvious that response times become significantly slower in lower grey levels. In addition, the vertically aligned LCs, except for LCs near patterned electrodes, collide together by unwanted interfering fields. This results in a slower rising time and a stronger grey scale dependency. In order to improve this slow response time in the PVA mode, overdriving technologies including dynamic capacitance compensation (DCC)[12,13)] and DCC II[14,15)] have been proposed. However, those technologies lead to the additional cost in device fabrications. Considering τ_{off}, when the LC deformation is associated with only K_3, it is advantageous to achieve a faster decaying time because K_3 is larger than K_1 (splay) and K_2 (twist).[16)] However, due to the collision between LCs, LC deformation is also associated with splay and twist.

Based on the deep understandings of electro-optic characteristics of the PVA mode, it is possible to optimize the best conditions for high transmittance, low driving voltage, and fast response time. Theoretically, the LC director should tilt downward in four different directions with $\phi(V) = \pi/4$ and the pure bend deformation should be achieved by defining surface tilt angles in each domain over whole cell area without the collisions between LC domains.

3. Experimental Procedure

The PVA cell having a defined pretilt angle is fabricated using RM monomers mixed with LC. Its fabrication process is illustrated as schematic drawings in Fig. 2. At first, the RM monomer (Merck RM-257) and the photo initiator (Ciba Irgacure-651) were added into a superfluorinated LC mixture. The superfluorinated LC mixture with a negative dielectric anisotropy $\Delta\varepsilon = -4$ and a birefringence $\Delta n = 0.077$ at $\lambda = 589$ nm was purchased from Merck and used as received. The homogenous mixture was injected into the PVA cell with the cell gap of 3.8 μm by a capillary force. Vertical alignment layers were applied on the substrates with patterned electrodes, as illustrated in Fig. 2. In order to minimize the ambient UV-exposure, all these processes were carried out in a dark room and the cell was preserved in the dark room right before the UV-curing process.

Without applying an electric field, RM monomers and LCs are vertically aligned due to the vertical alignment layers [Fig. 2(a)]. When an applied voltage (60 Hz) with a square wave larger than the Freedericksz transition voltage is applied to the cell, RM monomers as well as LCs are slightly tilted with respect to the surface normal, as described in Fig. 2(b). While maintaining the applied electric field, UV-light was exposed to the PVA cell [Fig. 2(c)]. Through this UV-curing process under a certain electric field, RM monomers are polymerized with a defined pretilt angles with respect to the surface normal, and this pretilt angles permanently sustain even after removing the applied voltages [Fig. 2(d)]. Utilizing this simple process, the defined pretilt angles could be controlled on surfaces of vertical alignment layers even without rubbing the substrates.[17,18)]

The defined pretilt angle of the existence of RM and its surface morphology of cured cell by RM monomer depending on the curing intensity was also studied by applying a square wave voltage which was larger than the threshold voltage. Without changing the total curing amount (about 437 J at the wavelength of 365 nm) and the content of RM (0.1 wt %), three different PVA cells were prepared by radiating UV light with different intensities for different times: 246.3 mW/cm^2 × 30 min, 98.5 mW/cm^2 × 74 min, and 5.0 mW/cm^2 × 24 h, respectively. Furthermore, in order to understand how rubbed surface of vertical alignment layer affects formation of polymer networks on the surface by RM monomer, the electrically controllable birefringence (ECB) VA cells were prepared by same conditions with PVA cells. Here both surfaces of VA layer were rubbed in antiparallel direction by rubbing process without patterning electrode. Finally, an effect of concentration of RM monomer into the LC was also confirmed. The surface morphologies of cured cells prepared at different conditions were investigated using polarized optical micro-

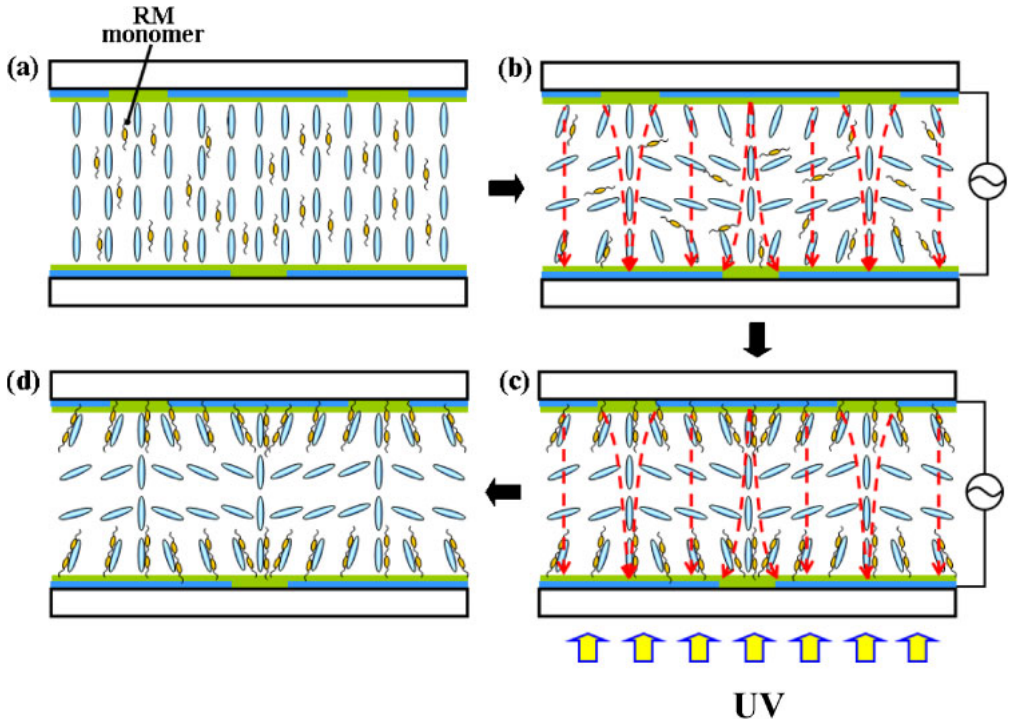

Fig. 2. (Color online) Schematic illustration of the surface-modified PVA cell exhibiting how the pretilt angle is formed using RM monomers.

scope (POM; Nikon E600) and field-emission scanning electron microscopy (FE-SEM; Hitachi S-4300SE). In order to observe the inside surface morphology of the cells, the sandwiched cells were separated and washed several times with *n*-hexane (96%), and then after drying the remained solvent the sample was coated with gold before SEM experiments.

4. Results and Discussion

The surface pretilt angles generated by the proposed approach could be controlled by the weight percent of RM, the UV-curing conditions and the intensity of electric fields during the UV-curing process. First, the proper amount of RM is critical not to generate any light scattering by refractive index mismatching between LC and polymerized RM and polymer itself by forming a comparable size to an incident wavelength. Second, the applied voltage during the UV exposure is one of the essential factors for this optimization because the surface pretilt is determined by the orientation of LCs near surface of substrates. Third, the initial intensity of UV curing is also a very important factor since it determines speed of diffusion of RM monomer to the surfaces and its polymerization although the total cured energy is the same.

Various approaches have been performed to find out optimal conditions of surface-modified PVA mode. At first, the LC textures of the conventional PVA cell were observed as a function of voltage, as shown in Fig. 3(a). As indicated, the PVA cell shows a perfect dark state under the cross polarized optical microscopy owing to the vertical alignment. With increasing voltage, the transmittance starts to occur. However, the thick dark disclination lines exist up to 2.8 V in the electrode patterned areas because the LCs in each domain tilt downward but in opposite directions so that they remain vertically aligned in these areas. With further

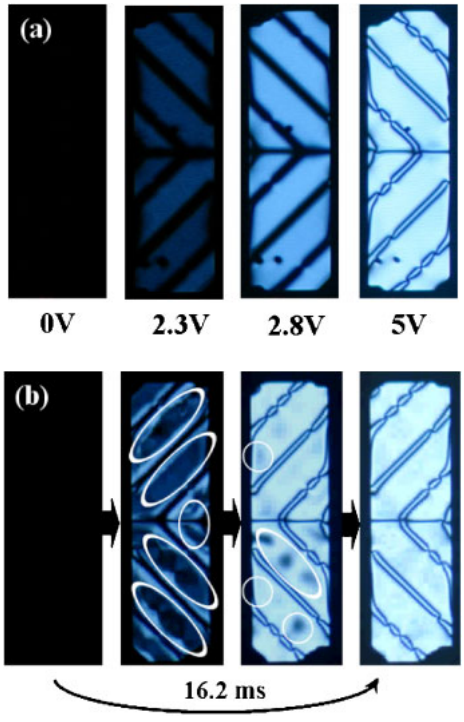

Fig. 3. (Color online) (a) Micro LC textures of the normal PVA cell as a function of applied voltages and (b) time-resolved LC textures with applied voltage of 5 V.

increasing voltage to 5 V, the thick line splits into two thin lines with defect points. In addition, time-resolved textures with 5 V shown in Fig. 3(b) show that the textures take a time to be stabilized. This means the LC reorientation in response to an electric field is not defined to deform in a desired direction. Therefore, defect points appeared between patterned electrodes, as described in Fig. 3(b). As a result, the PVA cell inevitably showed a slower rising time.

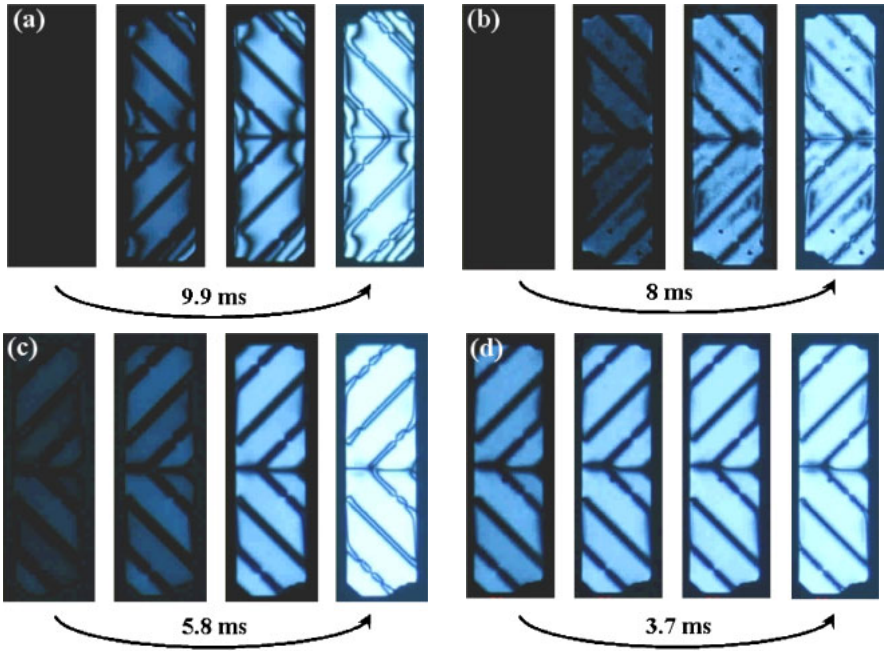

Fig. 4. (Color online) Time-resolved LC textures with applied voltage of 5 V: the surface-modified PVA cell cured at a specific voltage when the weight percent of RM monomer is in the specific condition: (a) 2.3 V, 0.1%, (b) 2.3 V, 1%, (c) 5.3 V, 0.1%, and (d) 5.3 V, 1%, respectively.

In order to prove this speculation and to overcome these problems, the concentration of RM monomer was varied from 1 to 0.1%, and the applied voltage was changed from 2.3 to 5.3 V during UV-curing process. The threshold voltage (T_{10}) which transmittance changed from 0 to 10% was 2.3 V, and the 5.3 V which transmittance changed from 0 to 90% was operation voltage (T_{90}). Figures 4(a)–4(d) showed time-resolved LC textures when RM monomer of 0.1% irradiated by UV at 2.3 V, RM of 1% irradiated at 2.3 V, RM of 0.1% irradiated at 5.3 V, and RM of 1% irradiated at 5.3 V, respectively. The whole surface-modified PVA cells of Fig. 4 showed a much faster rising time than a conventional PVA cell. In this case, a UV incident light of 365 nm with 5.0 mW/cm^2 was applied for 24 h during the UV-curing process.

As shown in Fig. 4(a), the initial LC texture in the surface-modified PVA cell cured at 2.3 V provided a perfect dark state like a conventional PVA cell [Fig. 3(a)]. However, the disclination lines causing the poor transmittance existed between the patterned electrodes in the whole range of grey scales, and the driving voltage was still higher than that of the conventional PVA cell. This unsatisfactory electro-optic performance of this PVA cell could be explained by the following phenomena. Generally, at a low grey level in the chevron structures, LCs around signal lines and pixel edges are tilted down to $\phi(V) \neq \pi/4$, which is resulted from the pixel edges and the additional electric field generated around signal lines. Therefore, when RM monomers were cured just above the threshold voltage, the azimuthal direction of surface pretilt angle of LCs could be fixed at $\phi(V) \neq \pi/4$. Based on this theoretical background, this fatal drawback, the generation of disclination lines shown in Fig. 4(a), can be avoided by increasing the curing electric voltage. Similar to the case of Fig. 4(a), Fig. 4(b) exhibited a poor transmittance and an undesired texture was generated due to the network formed by the addition of excessive RMs during the UV-curing process.

In the surface-modified PVA cell cured by UV at 5.3 V [Fig. 4(c)], the disclination lines observed in Fig. 4(a) were no longer existed. However, the cell retardation value is still not small enough to prevent a light leakage along the normal direction in the absence of an electric field. This should be due to the high pretilt angle generated during the UV-curing process at 5.3 V. When the excess amount of RMs (1%) at the operation voltage of 5.3 V was applied during the UV-curing process [Fig. 4(d)], the light leakage was severe compared with Fig. 4(c). This could be due to the fact that denser networks formed because of the excess amount of RMs at a high electric voltage.

The experimental observations as shown in Figs. 3 and 4 clearly indicate that the electro-optic performance of the surface-modified PVA cell is strongly dependent on both the concentration of RM and the UV-curing voltages. Therefore, it is essential to find the optimum condition of the UV-curing condition which of electric voltage between 2.3 and 5.3 V at the proper concentration of RM such as 0.1%.

Figure 5 shows the voltage–transmittance curves according to various UV-curing electric voltages when the concentration of RM monomer was fixed as 0.1%. In the Fig. 5, voltage–transmittance curves of the surface-modified PVA cells cured at 2.3 and 5.3 V showed similar trends as mentioned above in Fig. 4. The surface-modified PVA cell, which was prepared at the intermediate UV-curing electric voltage such as 3.7 V showed little light leakage and a slightly decreased threshold voltage with an increased transmittance due to the appropriately defined pretilt angle.

In order to confirm whether the stability of voltage-dependent LC reorientation is improved in the device with the defined pretilt angle or not, time-resolved LC textures of the conventional PVA cell and the surface-modified PVA cell UV-cured at 3.7 V were monitored by applying two different voltages to reach the transmittance of 50% (T_{50}) and 90% (T_{90}) of the maximum transmittance. The results were further compared with those of the conventional PVA

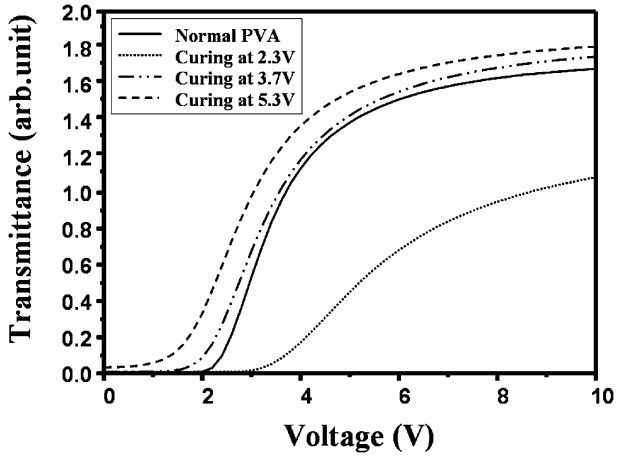

Fig. 5. Voltage–transmittance curves according to various curing voltages when the weight percent of RM monomer is fixed at 0.1%.

cell and represented in Fig. 6. In the conventional PVA cells at T_{50} and T_{90}, the instantaneous collisions between patterned electrodes are clearly observed before the stabilization of LC textures in both grey scales. These instantaneous collisions generated defects such as dark lines and spots during switching, which are emphasized with white circles in Figs. 6(a) and 6(b). By introducing a defined pretilt angle in the surface-modified PVA, undesired instantaneous collisions were successfully eliminated, as shown in Figs. 6(c) and 6(d). It is worth noting that the transmittance of the surface-modified PVA cell fabricated at the UV-curing voltage of 3.7 V was continually changed with respect to the time while maintaining the same texture. When the voltage was applied in the conventional PVA cell, it took 34.0 ms for T_{50} and 16.2 ms for T_{90}, respectively, in order to reach the stabilized LC textures. The rising response times in the surface-modified PVA cell UV-cured at 3.7 V were dramatically reduced to 17.1 ms for T_{50} and 4.1 ms for T_{90}. These encouraging results demonstrated that the surface-modified PVA cell with a defined pretilt angle can minimize the instantaneous collisions between LC domains, resulting in the shorter rising response time.

Furthermore, the rising and decaying response times of the surface-modified PVA cells UV-cured from 3.1 to 5.3 V measured according to changing grey scales were compared with those of the normal PVA cell. The results are represented in Figs. 7(a) and 7(b). The rising response times of the surface-modified PVA cells were twice faster than those of the conventional PVA cell. The surface-modified PVA cell UV-cured at 3.7 V showed a similar decaying response time compared with the conventional PVA cell while the surface-modified PVA cell UV-cured at 5.3 V exhibited a slower decaying response time. This could be due to the fact that the UV-curing voltage of 5.3 V was so high that the high pretilt angle with respect to surface normal was generated.

Based on the systematic experimental observations by tuning the UV-curing electric voltages, it was realized that electro-optic performances such as threshold voltage, transmittance and response time were optimized by introducing a proper defined pretilt angle on the surfaces. However, there is a remaining challenge in the surface-modified PVA cell: how can the light leakage in the dark state be minimized? The light leakages in the dark state can sacrifice the high contrast ratio at the normal direction, one of the main advantages of the PVA mode.

The light leakages in the dark state in the surface-modified PVA cell were evaluated according to the UV-curing electric voltages at a constant RM monomer concentration of 0.1%. Figures 8(a)–8(c) represent optical textures of a normal PVA cell, a surface-modified PVA cell at 3.7 and 5.3 V, respectively, taken under cross polarized optical microscopy (Nikon) with the sensitivity of 2. The light leakages in the dark state of the PVA cell were continuously increased by increasing the defined pretilt angles.

Table I summarized the contrast ratio according to UV-curing electric voltages when the concentration of RM

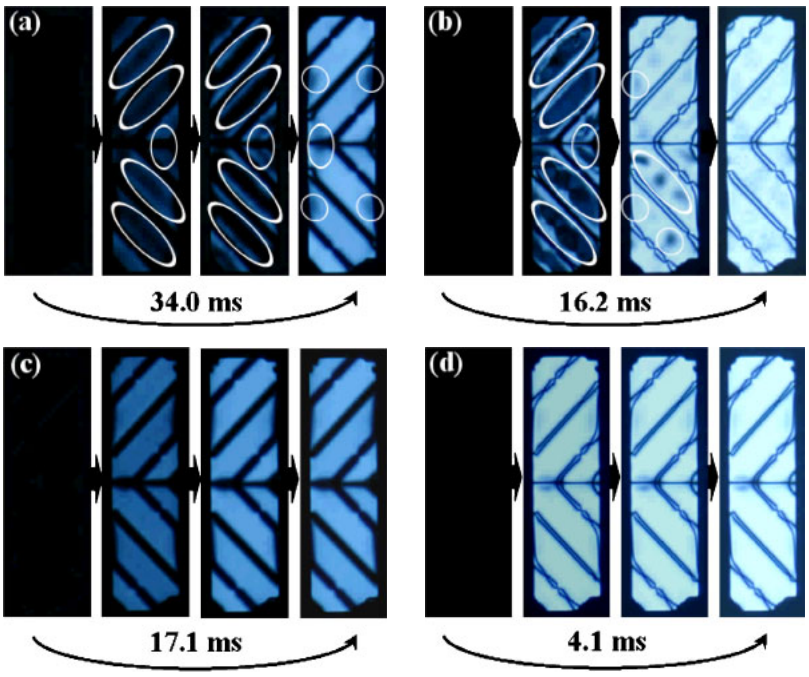

Fig. 6. (Color online) Time-resolved LC textures for comparison of LC dynamics responding to the applied voltages to reach T_{50} and T_{90} of maximal transmittance: (a) and (b) in the normal PVA cell and (c) and (d) in the surface-modified PVA cell cured at 3.7 V when the weight percent of RM monomer is 0.1%, respectively.

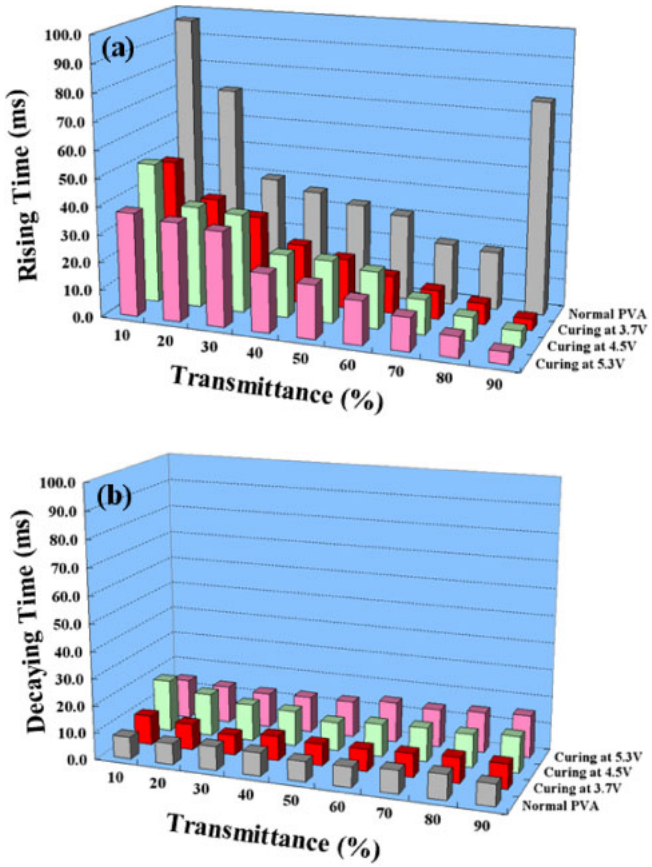

Fig. 7. (Color online) Comparison of (a) rising and (b) decaying grey level response times between the normal and the surface-modified PVA cells when the weight percent of RM monomer is 0.1%.

monomer was 0.1%. Contrast ratio of the surface-modified PVA cells with a defined pretilt angle was similar to that of the conventional PVA cell until the UV-curing voltage reached up to 3.1 V. However, it was decreased when the UV-curing electric voltage was above 3.7 V. Therefore, we can conclude that the defined pretilt angle is one of the important factors to minimize the light leakage without expense of the high contrast ratio at normal direction. The journey to improve the electro-optic performances of the surface-modified PVA mode should be continued.

In order to study the defined pretilt angles of cured RM by morphological observations, PVA cells were prepared by

Table I. Contrast ratio according to various curing voltages when the weight percent of RM monomer is 0.1%.

Sort of PVA	Normalized CR
Normal PVA	1
Curing at 3.1 V	1
Curing at 3.7 V	0.9
Curing at 4.5 V	0.67
Curing at 5.3 V	0.23

radiating UV light with higher intensities than the optimum value (5.0 mW/cm^2) and their POM. As shown in Fig. 9, three different PVA cells are prepared at different curing intensities: 246.3 mW/cm^2 [Fig. 9(a)], 98.5 mW/cm^2 [Fig. 9(b)] and 5.0 mW/cm^2 [Fig. 9(c)]. Compared to the PVA cells fabricated at the optimum intensity of UV [Fig. 9(c)], PVA cells which were prepared by radiating UV light with higher intensities [Figs. 9(a) and 9(b)] exhibited polymer branched rods in the range of 20–50 μm in length with the thickness of several micrometers. This can be explained by a phenomenon that UV curing reaction can be accelerated by increasing the UV intensity. The generated polymer rods bigger than the wavelength of light can induce light-leakage in the dark state due to the light scattering. The polymer branched rods lied down along the tilted direction of the LC, which is the perpendicular to the long axis of the LC and they exist mainly between patterned electrodes where the field intensity of non-patterned is stronger than that of the patterned area, as shown in Figs. 9(a) and 9(b). These morphological observations can be explained by the fact that the long axes of RM monomers are aligned parallel to the long axes of LCs under the electric field so that RM monomers are polymerized along the long axis of the LC. Consequently, owing to existence of additional polymer layer on surface, the pretilted angels are confined even without electric field.

Polymer branched rods generated by UV curing under the electric field were also investigated by FE-SEM with high resolution and their results were shown in [Figs. 10(a)–10(c)], which were prepared in the ECB-VA cells at different UV intensities of 246.3, 98.5, and 5.0 mW/cm^2, respectively. The surface morphologies of ECB-VA cells observed by FE-SEM were well matched with those represented in Fig. 9. The first two cases show polymer

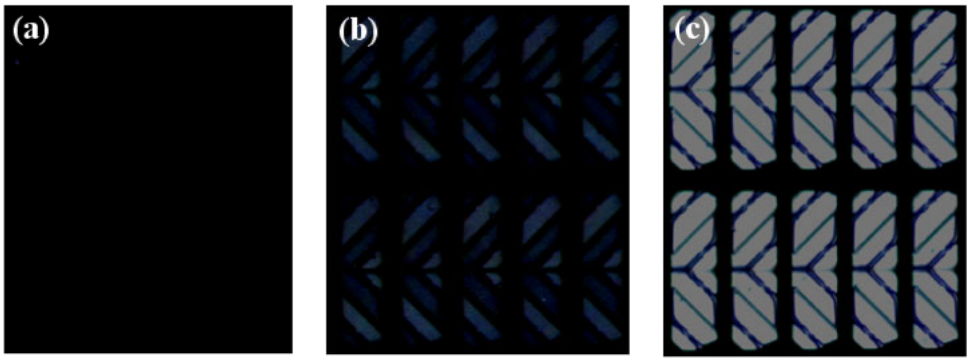

Fig. 8. (Color online) Light leakage in a dark state: (a) the normal PVA cell, (b) the surface-modified PVA cell cured at 3.7 V, and (c) the surface-modified PVA cell cured at 5.3 V when the weight percent of RM monomer is 0.1%.

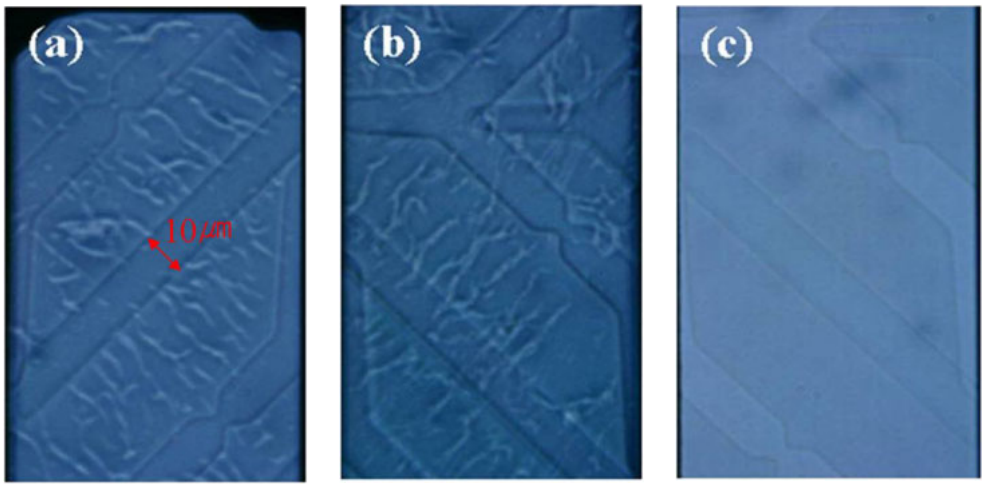

Fig. 9. (Color online) POM images of the inside surface of PVA cell prepared at different curing intensities: (a) 246.3 mW/cm^2 × 30 min, (b) 98.5 mW/cm^2 × 74 min, and (c) 5.0 mW/cm^2 × 24 h.

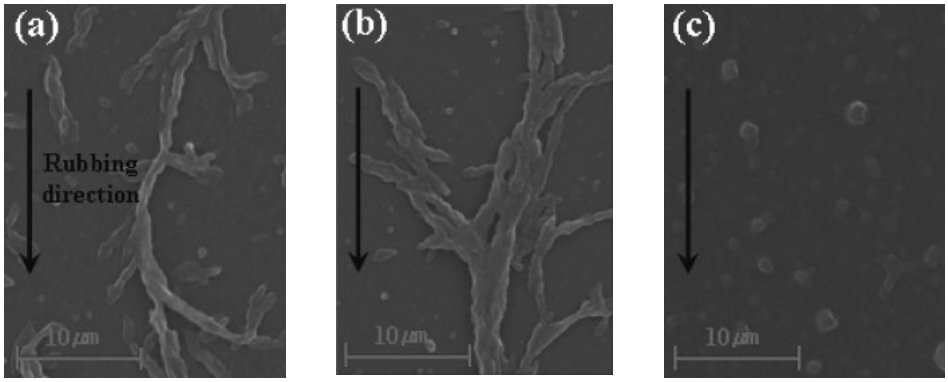

Fig. 10. SEM images of the inside surface of ECB-VA cell prepared at different curing intensities: (a) 246.3 mW/cm^2 × 30 min, (b) 98.5 mW/cm^2 × 74 min, and (c) 5.0 mW/cm^2 × 24 h.

branched rods but the latter case does not. It is noteworthy to remind the fact that rubbing process was not applied for the fabrication of PVA cells. In order to know the effect of rubbed alignment layer, the alignment layer of ECB-VA cells were rubbed along a certain direction before UV curing under an electric field. As expected, polymer branched rods were lied down along the rubbing direction, that is, the titled direction of LC, similar to the non-rubbed case of PVA cell. This result clearly indicates that the initial UV exposing intensity can be one of the dominating factors to determine the defined pretilt angles without forming polymer branched rods which could disturb the dark state of VA cells.

5. Conclusions

The surfaces of PVA mode were modified by using UV-curable RM. Moreover, their electro-optic characteristics and LCs dynamics were investigated according to the curing conditions. The pretilt angle with respect to the surface normal was optimized by controlling the concentration of the RM monomers, the initial UV exposing intensity and the UV-curing voltages. Through the careful experimental observations and analysis, it was realized that the optimized pretilt angle in the surface-modified PVA cell is the key factor to improve electro-optic characteristics without sacrificing the high contrast ratio at the normal direction. This surface-modified PVA mode with an optimized pretilt angle provided the well-defined reorientation of the LCs with respect to an electric field, which leads to significantly reduced threshold voltages and much faster response times in all grey scales compared with a conventional PVA mode. The defined pretilt angles were also confirmed by the surface morphological observations using FE-SEM and POM. Based on the systematic experimental observations, it was realized that for fine tuning a pretilt angle fabrication conditions of PVA cells, such as the concentration of the RM monomers, the UV-curing electric voltages and curing intensity, should be optimized. This newly proposed surface-modified technology can pave a new pathway in the development of LCDs using the PVA mode as well as a scientific insight of the molecular interactions on the surfaces.

Acknowledgements

This work was supported by LCD R&D center of Samsung Electronics Cooperation and partly supported by the Ministry of Commerce, Industry and Energy (MOCIE) and Korea Industrial Technology Foundation (KOTEF) through the Human Resource Training Project for Regional Innovation.

1) M. Schadt and W. Helfrich: Appl. Phys. Lett. **18** (1971) 127.
2) C. H. Park, S. H. Lee, J. K. Jeong, K. J. Kim, and H. C. Choi: Appl. Phys. Lett. **89** (2006) 101119.
3) M. Oh-e and K. Kondo: Appl. Phys. Lett. **67** (1995) 3895.
4) S. H. Lee, S. L. Lee, and H. Y. Kim: Appl. Phys. Lett. **73** (1998) 2881.
5) I. H. Yu, I. S. Song, J. Y. Lee, and S. H. Lee: J. Phys. D **39** (2006) 2367.
6) A. Takeda, S. Kataoka, T. Sasaki, H. Chida, H. Tsuda, K. Ohmuro, T. Sasabayshi, Y. Koike, and K. Okamoto: SID Int. Symp. Dig. Tech. Pap. **29** (1998) 1077.
7) K. H. Kim, K. Lee, S. B. Park, J. K. Song, S. N. Kim, and J. H. Souk: Proc. 18th Int. Display Research Conf. Asia Display, 1998, p. 383.
8) G.-D. Lee, J.-H. Son, Y.-H. Choi, J. J. Lyu, K. H. Kim, and S. H. Lee: Appl. Phys. Lett. **90** (2007) 033509.
9) S. S. Kim, B. H. Berkeley, and T. S. Kim: SID Int. Symp. Dig. Tech. Pap. **37** (2006) 1938.
10) S. G. Kim, S. M. Kim, Y. S. Kim, H. K. Lee, S. H. Lee, G. D. Lee, J. J. Lyu, and K. H. Kim: Appl. Phys. Lett. **90** (2007) 261910.
11) H. Wang, T. X. Wu, X. Zhu, and S.-T. Wu: J. Appl. Phys. **95** (2004) 5502.
12) K. H. Kim, J. J. Ryu, S. B. Park, J. K. Song, B. W. Lee, J. S. Byun, and J. H. Souk: Proc. 1st Int. Meet. Information Display, 2001, p. 58.
13) B. W. Lee, D. S. Sagong, and G. H. Jeong: SID Int. Symp. Dig. Tech. Pap. **32** (2001) 1106.
14) B. W. Lee, C. Park, S. Kim, M. Jeon, J. Heo, D. Sagong, J. Kim, and J. Souk: Proc. 7th Int. Display Workshops, 2000, p. 1153.
15) J. K. Song, K. E. Lee, H. S. Chang, S. M. Hong, M. B. Jun, B. Park, S. S. Seomun, K. H. Kim, and S. S. Kim: SID Int. Symp. Dig. Tech. Pap. **35** (2004) 1344.
16) S.-T. Wu and D.-K. Yang: *Reflective Liquid Crystal Displays* (Wiley, New York, 2001).
17) K. Hanaoka, Y. Nakanishi, Y. Inoue, S. Tanuma, Y. Koike, and K. Okamoto: SID Int. Symp. Dig. Tech. Pap. **35** (2004) 1200.
18) S. G. Kim, S. M. Kim, Y. S. Kim, H. K. Lee, S. H. Lee, J.-J. Lyu, K. H. Kim, R. Lu, and S.-T. Wu: J. Phys. D **41** (2008) 055401.